ARTICLE NO. 79-1548R

J80-178

Development and Structure of a Rectangular Jet in a Multiple Jet Configuration

20007

A. Krothapalli,*
University of Oklahoma, Norman, Okla.
and
D. Baganoff† and K. Karamcheti‡
Stanford University, Stanford, Calif.

Results of hot-wire measurements in an incompressible jet issuing from an array of rectangular lobes, equally spaced with their small dimensions in a line, are presented. The quantities measured include mean velocity and the Reynolds stress in the two central planes of the jet at stations covering up to 115 widths (small dimension of the lobe) downstream of the nozzle exit. Measurements are carried out on a single rectangular free jet and on the same jet in a multiple jet configuration. In the case of a multiple jet, the flowfield for downstream distance X greater than $60D$ (D = width of the lobe) resembles that of a jet exiting from a two-dimensional nozzle with its short dimension being the long dimension of the lobe. The field of turbulence is found to be nearly isotropic in the plane containing the small dimension of the lobes for X greater than $60D$.

Nomenclature

AR	= aspect ratio (L/D)
D	= width (small dimension) of the lobe
L	= length (long dimension) of the lobe
S	= spacing between the lobes
U	= mean velocity component in the X-direction
U_c	= mean velocity component along the centerline of the jet in the X-direction
U_0	= mean velocity component in the exit plane of the jet in the X-direction
u	= fluctuation velocity component in the X-direction
u_{rms}	= $\sqrt{u^2}$ = rms velocity fluctuations in the X-direction
$\tilde{u}$	= $\sqrt{u^2}/U_c$ (normalized rms velocity fluctuation in the X-direction)
V	= mean velocity component in the Y-direction
v_{rms}	= $\sqrt{v^2}$ = rms velocity fluctuation in the Y-direction)
$\tilde{v}$	= $\sqrt{v^2}/U_c$ (normalized rms velocity fluctuation in the Y-direction)
W	= mean velocity component in the Z-direction
w	= fluctuation velocity component in the Z-direction
$\tilde{w}$	= $\sqrt{w^2}/U_c$ (normalized rms velocity fluctuation in the Z-direction)
$\overline{uv}, \overline{uw}, \overline{vw}$	= components of the turbulent shear stress tensor
X	= coordinate along the jet axis
Y	= coordinate along the small dimension of the lobe
$Y_{1/2}$	= local half-width of the U profile along the Y axis
Z	= coordinate along the long dimension of the lobe
$Z_{1/2}$	= local half-width of U profile along the Z axis
η	= Y/X
ξ	= Z/X

Presented as Paper 79-1548 at the AIAA 12th Fluid and Plasma Dynamics Conference, Williamsburg, Va., July 24-26, 1979; submitted Sept. 17, 1979; revision received Feb. 19, 1980.

Index category: Jets, Wakes, and Viscid-Inviscid Flow Interactions.

*Assistant Professor, School of Aerospace, Mechanical, and Nuclear Engineering. Member AIAA.

†Professor, Joint Institute for Aeronautics and Acoustics, Dept. of Aeronautics and Astronautics. Member AIAA.

‡Professor and Director, Joint Institute for Aeronautics and Acoustics, Dept. of Aeronautics and Astronautics. Fellow AIAA.

Introduction

MULTIPLE jets are used in a wide variety of engineering applications, for example, thrust augmenting ejectors for VTOL/STOL aircraft. The configuration of interest here is an array of rectangular lobes in a line, as shown in Fig. 1. Very few investigations have been reported in the literature regarding the structure and development of multiple jets, in particular the present configuration. Early work on this subject was done by Corrisin[1] who studied the flow from seven parallel slot nozzles in a common wall with emphasis on flow stabilization methods. Laurence and Benninghoff[2] and Laurence[3] studied the flow emanating from four rectangular lobes. Most of the emphasis in these studies was placed on finding a noise mechanism rather than on the detailed structure of the flowfield. The gross characteristics of the flowfield emanating from rectangular lobes in the line was recently reported by Marsters.[4] The flow emanating from a series of closely spaced holes in line has been studied experimentally by Knystautas.[5] Overall aerodynamic studies have been made by Aiken[6] on an ejector with multiple rectangular lobes with various spacing-to-width ratios and nozzle dimensions. In all the studies mentioned, most of the measurements were made on mean flow rather than on the detailed turbulence structure. The purpose of the present paper is to present and discuss the results of experiments with a multiple jet configuration and, thus, add to the understanding of its fluid mechanical structure. The data also provide numerical analysts with a basis on which a computational model can be built. The experimental investigation presented here constitutes a part of a larger program on turbulent mixing of multiple rectangular jets being studied at Stanford.

The characteristics of the flowfield depend upon the aspect ratio of the lobe, inlet geometry of each lobe, the magnitude of the turbulence intensity at the exit plane of each lobe, the Reynolds number at the lobe exit, and spacing between the lobes. In the present investigation, a lobe of aspect ratio 16.7 was chosen. The spacing between the lobes was $8D$ (D being the small dimension of the lobe). These parameters were chosen to be consistent with the nozzle used by Aiken.[6] Inlet

geometry of the nozzle was designed specifically to obtain minimum turbulence level at the exit plane. The velocity profile at the exit plane of each lobe was flat with a laminar boundary layer at the walls. A mean velocity of 60 m/s was maintained at the exit plane of each lobe. This results in a Reynolds number of 1.2×10^4 based on the width of the lobe.

Measurements were made using hot-wire anemometry. They include the mean velocities and turbulent intensities for the three components of velocity and the turbulent shear stresses $\overline{uv}$ and $\overline{uw}$ (see Fig. 1). Most of the detailed measurements were made in the two perpendicular central planes of the center lobe.

Apparatus, Instrumentation, and Procedure

A blow-down air supply system was used to provide the airflow to a cylindrical settling chamber whose dimensions are 1.75 m long and 0.6 m in diameter. The facility is designed to provide sonic conditions at the exit plane of the nozzle for other experiments. Before reaching the nozzle, air passes through an adapter which contains six screens set 5 cm apart to reduce disturbances at the inlet of the nozzle. The ratio of areas between the adapter and the nozzle is 90, which is exceptionally large when compared with the contraction ratio for conventional wind tunnels. The turbulence level at the exit of the nozzle was about 0.3% at 60 m/s. The long (L) and short (D) dimensions of the rectangular lobe exit are 50 mm and 3 mm, respectively. The spacing (S) between the lobes is 24 mm. Each lobe exit is preceded by a 40-mm-long rectangular (50 mm × 3 mm) channel. The experimental facility and the model are described in detail by Krothapalli.[7] The exit velocity of the jet was maintained to an accuracy better than 1%.

Measurements were made with DISA 55M01 constant temperature anemometers in conjunction with DISA 55D10 linearizers. Most of the measurements were made using either an X-wire or a single wire. These wires were manufactured by DISA and constructed from 5-μm platinum-coated tungsten wire with an active length of 1.2 mm. When X-probes were used, each of the attenuators on the linearizers was adjusted to give the same output for each wire when the probe was perfectly aligned with the stream. The yaw sensitivity of each wire was then checked. The simple cosine law was used to decompose the velocities. From the calibration, the use of an X-wire probe in turbulent flows was found to be limited to situations where the angular rotation of the velocity vector does not exceed ±25 deg. The response of the hot wire was assumed linear, and no corrections resulting from higher order terms were applied. The error in turbulence measurements caused by assuming the normal component or cosine law cooling, and neglecting the nonlinearities caused by high intensity turbulence, was estimated by Champagne and Sleicher.[16] For the quantities measured (rms intensities and turbulent shear stresses), the error ranges from 0-17%.

The signals were then passed through two DISA-type 55D31 digital voltmeters, DISA 55D35 rms units, and TSI model 1076 voltmeteres to get the mean and rms values. The integration times on these instruments can be selected in discrete steps from 0.1 to 100 s. Measurements of correlations were made using an HP 3712A correlator. For most of the results presented, random errors were estimated to be of the order of 2 ~ 3% and a systematic error in the axial component of velocity (due to cosine law decomposition) of approximately 5% was present.

A Cartesian coordinate system (X, Y, Z) is chosen with its origin located at the center of the center lobe, as shown in Fig. 1, with the X axis oriented along the centerline of the jet. Hot-wire traverses were made in the two central X,Y and X,Z planes at various streamwise (X) locations, covering up to 115D. Unless otherwise stated, all the data presented here were taken with the X-wire pobe. The experiment was conducted in two parts. In the first part, measurements were made on the center lobe with all the other lobes blocked. In the second part, measurements were made on the center lobe with all five lobes blowing. Most of the measurements in both the cases were made on the two central planes of the center lobe. Mean velocity measurements were made across the center three jets in order to establish the symmetry of the flow about their central planes; however, only the data for each half plane of the center lobe will be presented.

Results and Discussion

General Features of the Flowfield

On the basis of the present investigation and the results reported by Sforza et al.,[8,9] Sfeir,[10,11] and those summarized

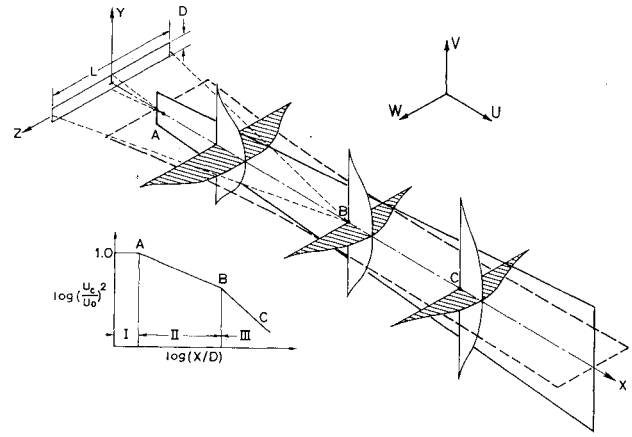

Fig. 2 Schematic representation of flowfield of a rectangular free jet.

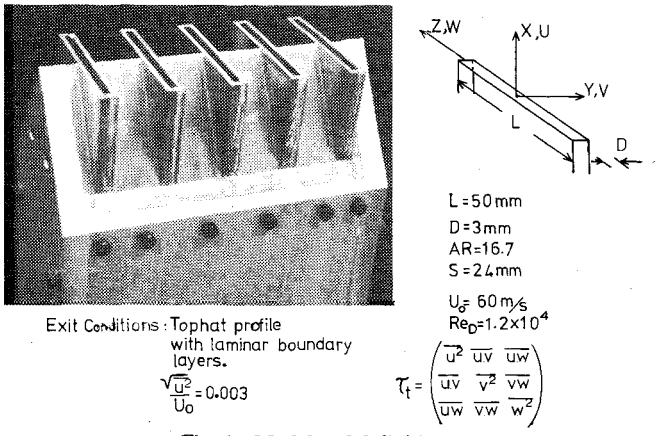

Fig. 1 Model and definitions.

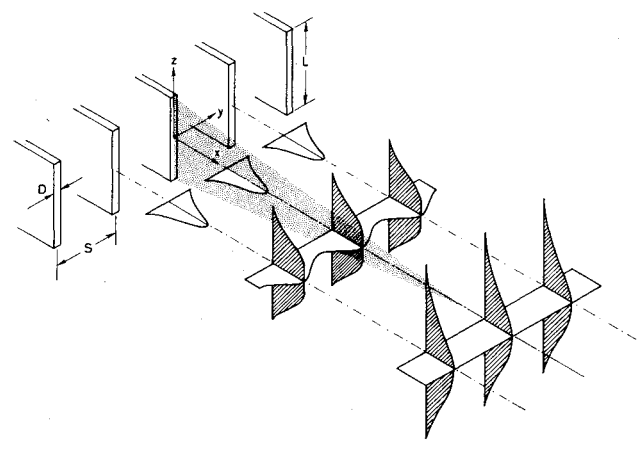

Fig. 3 Schematic representation of flowfield of a multiple free jet.

by Rajaratnam,[12] the flowfield of a rectangular free jet may be represented schematically, as shown in Fig. 2. Also shown in the figure (as an insert) is the variation of $\ell n(U_c/U_0)^2$ with $\ell n(X/D)$. The three regions, as shown in the figure, may be classified as follows: the first region is referred to as a potential core region in which the axial velocity is constant; the second region denoted by AB, in which the velocity decays at a rate roughly the same as that of a planar jet, will be referred to as the two-dimensional region; and the third region downstream of B, in which the velocity decays at nearly the same rate as that of an axisymmetric jet, will be referred to as an axisymmetric region. The two-dimensional type region originates at about the location where the two shear layers in the X,Y plane (containing the short dimension of the nozzle) meet. Correspondingly, one may expect the axisymmetric region to originate at a location where the two shear layers in the X,Y plane (containing the long dimension of the nozzle) would meet.

Profiles of the mean axial velocity in the X,Y and X,Z planes at three different locations are shown in the schematic of flow structure in Fig. 2. In regions I and II, the width of the jet in the X,Z plane is greater, as expected, than the width in the X,Y plane. At B, the widths in both planes are about the same. In region III, the width in the X,Y plane becomes larger than that in the X,Z plane.

The solid and dashed lines shown in the flow schematic depict the loci of maximum turbulent stresses in the two planes being considered. Detailed discussion of the flow structure with supporting measurements is given by Krothapalli et al.[13]

A schematic of the flowfield of a multiple rectangular free jet is shown in Fig. 3. Mean velocity profiles in the two central planes for the center three lobes are shown in the figure. For the configuration tested ($S=8D$, $AR=16.7$), the flow from each lobe does not exhibit any mutual interaction for X less than $15D$. Complete merging of the jets (i.e., individual jets lose their identity) is observed for X equal to $60D$, as indicated by a flat velocity profile across the lobes. The mean velocity profile in the central X,Z plane at different downstream locations exhibits characteristics similar to that of a single free jet. The shaded region is an attempt to show the pseudo-potential core region, after which the jet acts like a single two-dimensional jet with its minor axis being along the X axis.

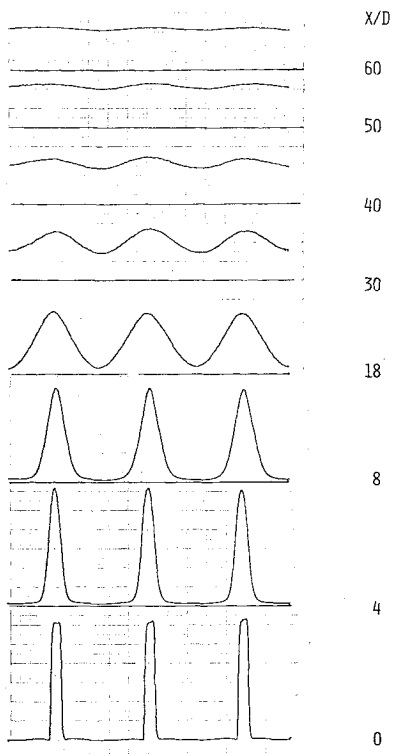

Fig. 4 Axial mean velocity profiles across the center three jets.

Mean Velocities

Mean axial velocity profiles, for the case of multiple free jets, in the central X,Y plane for the center three lobes at various downstream locations covering up to X, equal to $60D$ are shown in Fig. 4. At the exit plane, top-hat profiles with equal mangitudes are found with very little secondary flow between the jets. Significant merging of the jets first seems to occur at a location of about $18D$. The flat profile establishes that complete mixing of the jets has occurred at a location of approximately $60D$. Velocity profiles are observed to be flat across the center three lobes for locations of $60D \lesssim X \lesssim 115D$.

For the configuration ($S=8D$, $AR=16.7$) studied, a significant region exists where the mean velocity profiles of the individual jets behave quite independently of each other. However, measurements for the case of two unventilated parallel jets, such as the ones studied by Miller and Cummings,[14] show a subatmospheric pressure region between the jets near the nozzle exit, and the two jets attract each other. To further examine this phenomenon, a short-time exposure (5 μs) schlieren picture was taken of the three center lobes and is shown in Fig. 5. Here, it is observed that the individual jets do not attract each other and mix with ambient air quite independently. The large scale structure which usually ap-

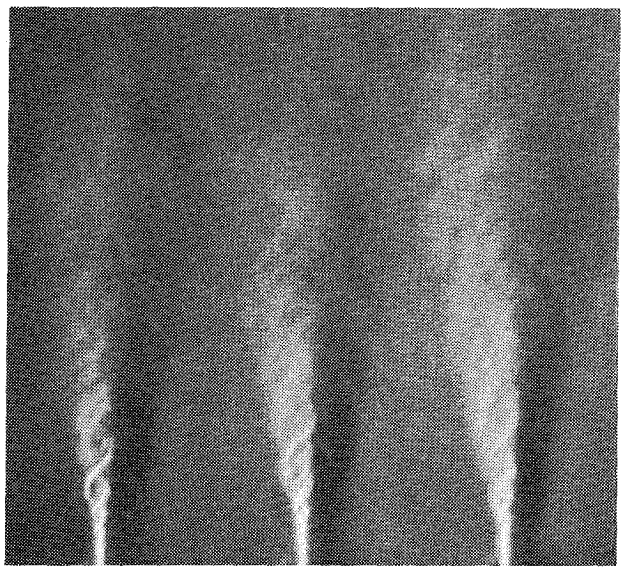

Fig. 5 Schlieren picture of a multiple free jet.

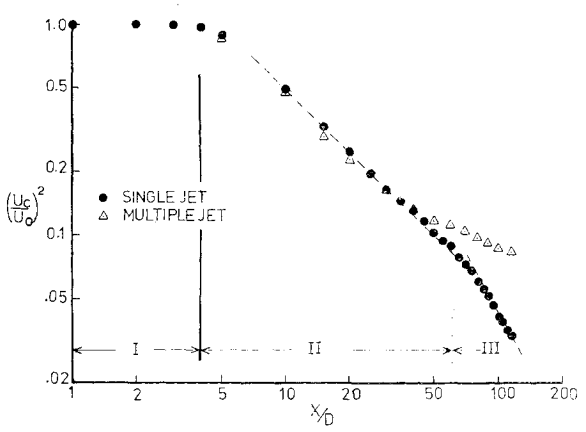

Fig. 6 The decay of the axial mean velocity along the centerline of the jet.

pears in the transition region of a jet can be seen in this picture (see Ref. 7 for details).

The decays of the square of the mean axial velocity with downstream distance for the two cases is shown in Fig. 6. The three regions noted in Fig. 2 are identified as the potential core region which ends at $3D$-$4D$, the two-dimensional jet-type region extending up to $60D$, and the axisymmetric jet-type region extending beyond $60D$. The decay for the case of a multiple free jet is almost identical to a single free jet up to X equal to $40D$. For X greater than $40D$, the decay is slower, as shown in the figure.

The normalized mean velocity profiles in the X, Y plane for the center jet from $Y=0$ to $Y=4D$ (midway between the two adjacent lobes) are shown in Fig. 7 for the three cases. The profiles upstream of the merging region are identical for the cases of a single jet and the multiple free jet, as depicted by the profiles at X equal to $10D$. A nearly flat profile is observed at $60D$.

The normalized mean velocity profile in the central X,Z plane for the case of the multiple free jet are shown in Fig. 8

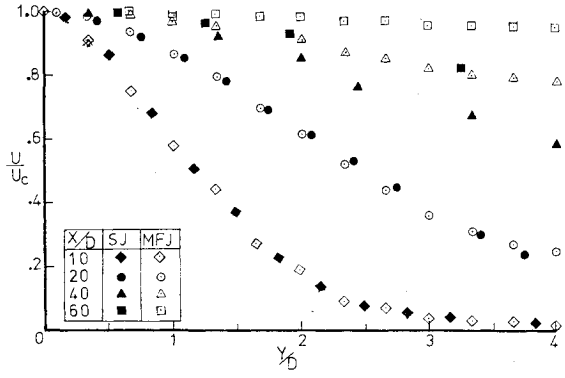

Fig. 7 Axial mean velocity profiles in the X, Y plane.

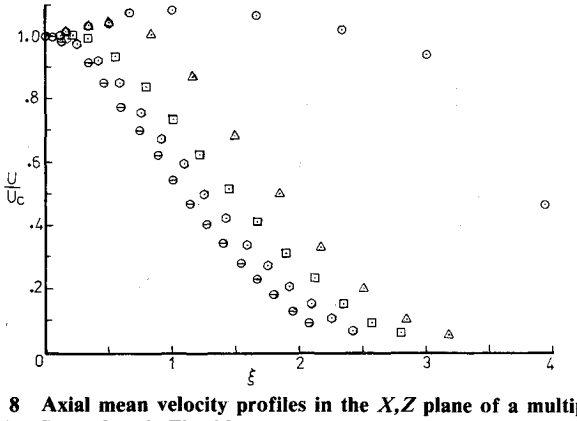

Fig. 8 Axial mean velocity profiles in the X,Z plane of a multiple free jet. Symbols as in Fig. 16.

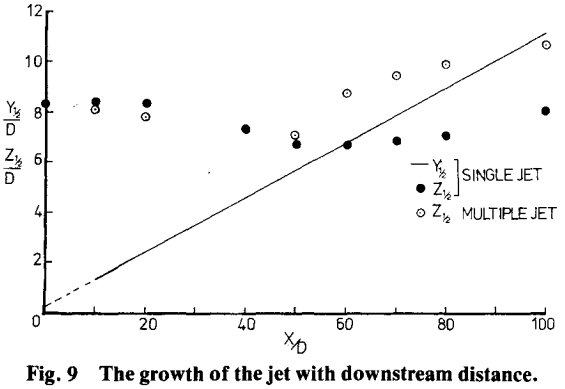

Fig. 9 The growth of the jet with downstream distance.

for various downstream locations. For X less than or equal to $40D$, the profiles exhibit a saddle shape with a maximum appearing near the centerline, and are identical to that of a single free jet when compared at their corresponding locations. Profiles for X greater than $40D$ in the multiple free jet case are broader than that of a single jet at their corresponding locations. To further examine this, the growth rate in the X,Z plane of the center jet in both the single and multiple free jet configurations are plotted with downstream distance in Fig. 9. The growth rate in the X,Y plane for a single jet is also included in the figure ($Y_{½}$ and $Z_{½}$ are the distances from the centerline of the jet to a location where the mean velocity is half of the centerline velocity along Y and Z axes, respectively). As one expects from the above discussion, the growth rate of the jet in the X,Z plane for both cases is almost identical up to X equal to $40D$. For X greater than $40D$, the growth rate in the multiple jet configuration is greater than that of a single jet. From these observations, it may be concluded that, for the spacing studied, the mutual interaction between the jets is strongly felt at about X equal to $40D$, while significant merging of the jets in the central X, Y plane occurs at X equal to $20D$.

Turbulent Intensities and Shear Stresses

The rms intensity for the axial component of velocity along the centerline of the jet for the two cases is shown in Fig. 10, along with the results (data represented by a solid line) of Gutmark and Wyganski[15] for a planar jet. The rms intensity is normalized with respect to the mean axial velocity at the exit rather than with the local mean centerline velocity. The rms values are almost identical in the two cases for X less than $40D$. For X greater than $40D$, the values for the multiple jets are less in magnitude than that of a single free jet. This substantial reduction in magnitude is the result of a mutual interaction between the adjacent jets. The results for a planar jet are shown for purposes of comparison and exhibit values higher than that of the single rectangular jet. It is felt that this difference can be attributed to different initial conditions in the two experiments.

We have observed that the values of v_{rms} and u_{rms} along the centerline have variations similar to u_{rms}. For X greater than $60D$, we have found $v_{\text{rms}} = w_{\text{rms}} \simeq 0.9\, u_{\text{rms}}$ for the case of the multiple free jet, which suggests isotropy along the centerline of the jet.

Figure 11 presents the profiles for $\tilde{u}(u_{\text{rms}}/U_c)$ in the X, Y plane for the case of multiple free jet and for different downstream locations. Profiles for X less than $20D$ are almost identical to a single free jet when compared at appropriate locations. For X greater than or equal to $60D$, the profiles become flat just as the mean velocity profiles. It was also found that the profiles of $\tilde{v}$ and $\tilde{w}$ for X greater than or equal to $60D$ are flat and equal in magnitude with $\tilde{u}$ at their corresponding locations. These profiles are shown in Figs. 12 and 13. This again suggests isotropy in the central X, Y plane.

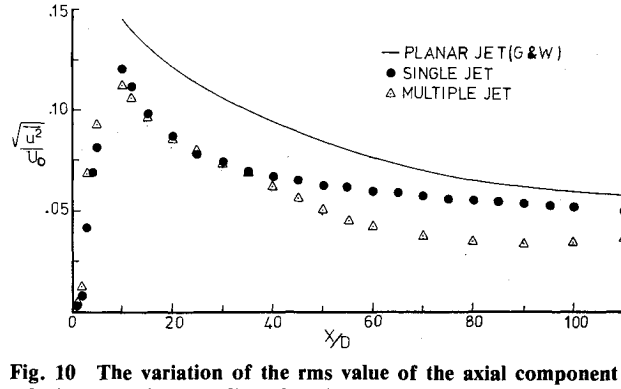

Fig. 10 The variation of the rms value of the axial component of velocity along the centerline of the jet.

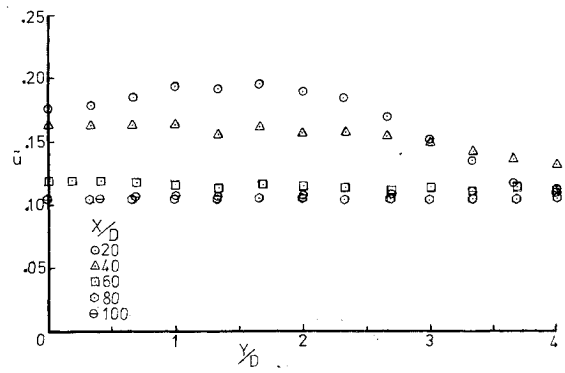

Fig. 11 The distribution of axial velocity fluctuation in the X, Y plane of a multiple free jet.

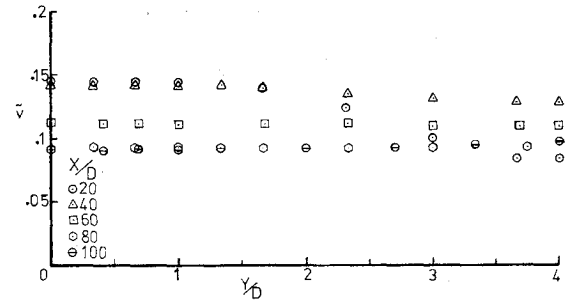

Fig. 12 The distribution of the lateral velocity fluctuations in the X, Y plane of a multiple free jet.

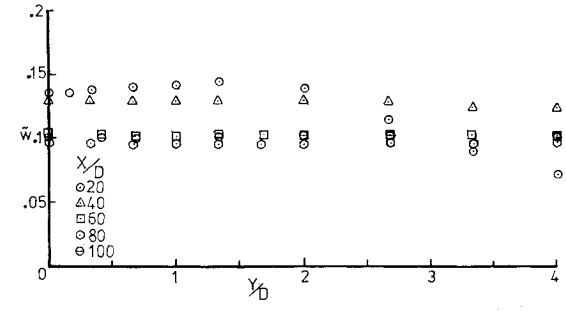

Fig. 13 The distribution of the transverse velocity fluctuations in the X, Y plane of a multiple free jet.

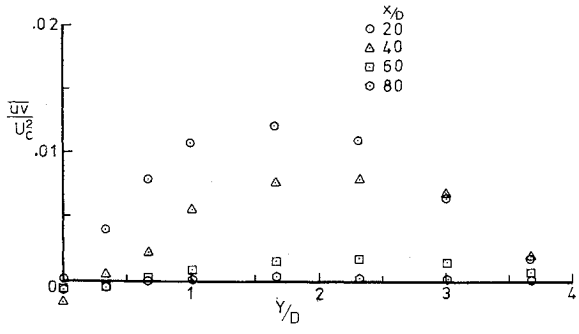

Fig. 14 The distribution of the turbulent shear stress in the X, Y plane of a multiple free jet.

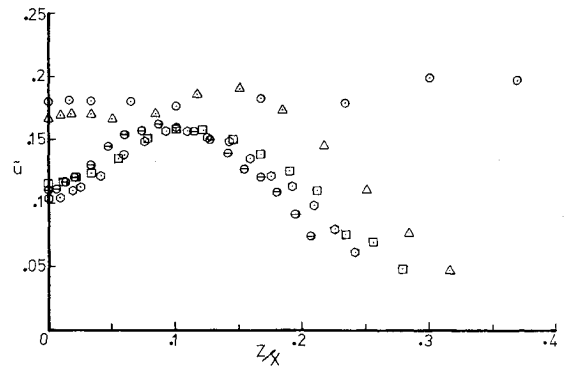

Fig. 15 The distribution of axial velocity fluctuations in the X, Z plane of a multiple free jet. Symbols as in Fig. 16.

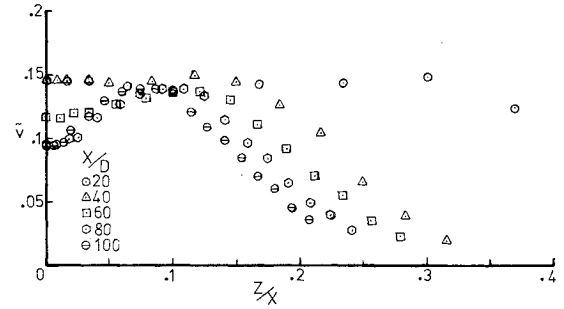

Fig. 16 The distribution of the lateral velocity fluctuations in the X, Z plane of a multiple free jet.

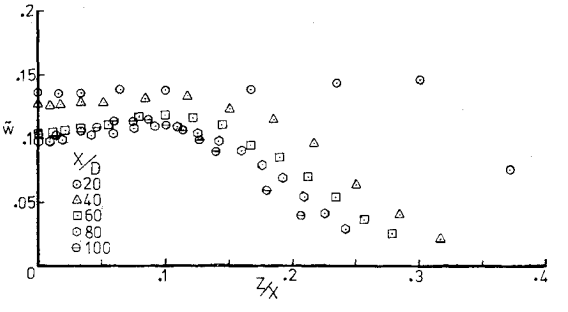

Fig. 17 The distribution of the transverse velocity fluctuations in the X, Z plane of a multiple free jet.

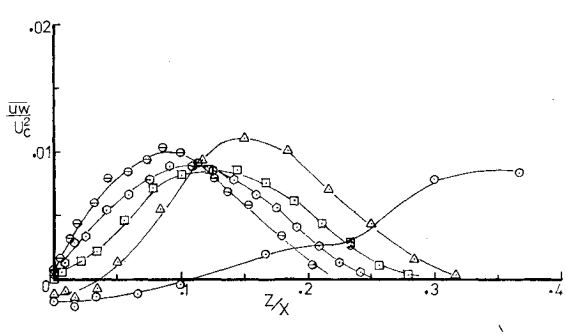

Fig. 18 The distribution of the turbulent shear stress in the X, Z plane of a multiple free jet. Symbols as in Fig. 16.

To examine further the degree of isotropy in the central X, Y plane, the normalized turbulent shear stress $\tilde{u}\tilde{v}\,(\overline{u\,v}\,/\,u_c^2)$ for different downstream locations are plotted in Fig. 14. For X equal to $20D$, the profile is quite similar to that of a single jet. For X greater than $60D$, the normalized stress is quite small in contrast to a single jet where it varies only slightly with downstream distance. The normalized turbulent shear stress $\tilde{u}\tilde{w}$ in the X, Y plane is found to be negligible for all downstream stations studied.

The profiles of $\tilde{u}$ in the X, Y plane, for the case of multiple free jets and for various downstream locations covering up to $100D$, are shown in Fig. 15. For X less than $40D$, the profiles are similar to those for a single free jet. For X greater than or equal to $60D$, the profiles develop a pronounced saddle shape,

as shown in the figure. The appearance of a saddle shape profile in a jet usually indicates the end of the potential core. With this in mind, one may conclude that the flowfield appears as though it is emerging from a single two-dimensional slot with the width of the slot being the long dimension of the lobe. The shaded region in Fig. 3 was drawn to represent a pseudo-potential core for this equivalent two-dimensional jet which ends at X equal to about $60D$.

The profiles of $\bar{v}$ in the X,Z plane are shown in Fig. 16. For X greater than $60D$, the profiles exhibit a saddle shape. This further supports the above discussion. However, $\bar{w}$ profiles, which are shown in Fig. 17, do not exhibit a significant saddle shape, which is consistent with the observation of the profiles at the end of a potential core of a two-dimensional jet.

The normalized turbulent shear stress $\overline{uw}$ in the central X,Z plane, in the case of the multiple free jet, is plotted in Fig. 18. At each location X, the point of maximum shear stress corresponds to the point where the velocity gradient $(\partial U/\partial Z)$ and turbulent intensities are maximum. We again found that, when compared with that of a single free jet, the values of $\overline{uw}$ for X greater than $40D$ are less at corresponding locations. In addition, the magnitudes of $\overline{uv}$ are negligible in the central X,Z plane.

Conclusions

In the case of a single rectangular jet, the flow is characterized by the presence of three distinct regions when the decay of the square of the axial mean velocity is used to describe the flowfield. These regions are: the potential core region, a two-dimensional type region, and an axisymmetric region.

For the case of a ventilated array of rectangular jets having a spacing of $8D$, the following observations are made. Because the individual jets act quite independently of each other near the nozzle exit, the point at which the individual jets begin to merge can be estimated from data on the growth rate of a single jet. Far downstream, the flowfield appears as if it is emerging from a single two-dimensional slot with the width of the slot being the long dimension of a single lobe. The mutual interaction between the jets results in a lower turbulence level when compared to a single jet at corresponding locations.

Acknowledgment

This work was supported by NASA Ames Research Center.

References

[1] Corrisin, S., "Investigation of the Behavior of Parallel Two-Dimensional Air Jets," NACA W-90, 1944.

[2] Laurence, C. J. and Benninghoff, N. J., "Turbulent Measurements in Multiple Interfering Air Jets," NASA TN 4029, 1957.

[3] Laurence, C. J., "Turbulence Studies of a Rectangular Slotted Noise Suppressor Nozzle," NASA TND-294, 1960.

[4] Marsters, F. G., "Measurements in the Flow Field of a Linear Array of Rectangular Nozzles," AIAA Paper 79-0350, Jan. 1979.

[5] Knystautas, R., "The Turbulent Jet from a Series of Holes in Line," *The Aeronautical Quarterly*, Vol. XV, Feb. 1964.

[6] Aiken, N. T., "Aerodynamic and Noise Measurements on a Quasi-Two Dimensional Augmenter Wing Model with Lobe-Type Nozzles," NASA TMX-62,237, Sept. 1973.

[7] Krothapalli, A., "An Experimental Study of Multiple Jet Mixing," Ph.D. Dissertation, Stanford University, Stanford, Calif., June 1979.

[8] Sforza, M. P., Steiger, H. M., and Trentacoste, N., "Studies on Three-Dimensional Viscous Jets," *AIAA Journal*, Vol. 4, May 1966, pp. 800-806.

[9] Trentacoste, N. and Sforza, M. P., "Further Experimental Results for Three-Dimensional Free Jets," *AIAA Journal*, Vol. 5, May 1967, pp. 885-891.

[10] Sfeir, A. A., "The Velocity and Temperature Fields of Rectangular Jets," *International Journal of Heat and Mass Transfer*, Vol. 19, 1975, pp. 1289-1297.

[11] Sfeir, A. A., "Investigation of Three-Dimensional Turbulent Rectangular Jets," AIAA Paper 78-1185, July 1978.

[12] Rajaratnam, N., *Turbulent Jets*, Elsevier, New York, 1976, pp. 267-271.

[13] Krothapalli, A., Baganoff, D., and Karamcheti, K., "Turbulence Measurements in a Rectangular Jet," AIAA Paper 79-0074, New Orleans, La., Jan. 1979.

[14] Miller, R. D. and Cummings, W. E., "Force Momentum Fields in a Dual Jet Flow," *Journal of Fluid Mechanics*, Vol. 7, No. 2, 1960, pp. 237-255.

[15] Gutmark, G. and Wygnanski, I., "The Planar Turbulent Jet," *Journal of Fluid Mechanics*, Vol. 73, Pt. 3, 1976, pp. 465-495.

[16] Champagne, H. F. and Sleicher, A. C., "Turbulence Measurements with Inclined Hot Wires, Pt. 2. Hot-Wire Response Equations," *Journal of Fluid Mechanics*, Vol. 28, Pt. 1, 1967, pp. 177-182.